DOI 10.1007/s11182-022-02700-7
Russian Physics Journal, Vol. 65, No. 5, September, 2022 (Russian Original No. 5, May, 2022)

INTEGRATED ANALYSIS OF MECHANICAL AND ACOUSTIC PROPERTIES OF MATERIALS

L. B. Zuev, M. V. Nadezhkin, and N. M. Mnikh

UDC 538.951, 539.37, 539.382.2

A model of evolution of the localized plastic flow of a solid is considered based on the idea of interaction of plastic flow carriers and signals of acoustic emission pulses originating during elementary plasticity acts. It is shown that the plastic flow is always localized on the macrolevel, and the volume localization takes forms of different autowave processes and is defined by the work hardening law.

Keywords: plasticity, deformation, defects, autowaves, failure.

INTRODUCTION

Studies of plasticity of metals and alloys performed in the previous years (for example, see [1]) showed that the obligatory and most important characteristic of plastic flow processes is their tendency to localization. It was established that at any stage of the process of changing the form of the material, the specific picture of localization center distribution – the localized plastic flow pattern – is spontaneously generated. The pattern is defined by the law of work hardening acting in the material. The observed localization patterns can be used as informative characteristics to predict the plasticity margin of deformable materials. This idea becomes even more attractive if we take into account that many physical properties of deformable media, in particular, acoustic ones, change upon plastic deformation.

For this reason, it is important to record simultaneously the mechanical and acoustic properties together with the localized plastic flow pattern. In this case, it should be born in mind that changes of the acoustic characteristics in a plastic flow typically do not exceed 10^{-4}–10^{-3}, so that recording of arising changes is difficult problem. Variations of the ultrasound propagation velocity accompanying changes in the composition, structure, and state of materials were detected and described in detail [2]. Later on, a great number of works were devoted to an analysis of the nature of the relationship between the acoustic properties of materials and the plastic deformation. The parallel study of the corresponding deformation laws demonstrated that small changes in the ultrasound propagation velocity in solids can be used as informative parameters. The approach developed in our works that relates the mechanical and acoustic properties of solids under plastic deformation also supports this idea. It is characterized by the elastic-plastic deformation invariant [1] and its consequences [3].

1. TEST STAND AND ITS CAPABILITIES

To develop and to confirm these ideas on the plastic flow dynamics, it was necessary to create a measuring stand to carry out mutually supplementing studies of the mechanical and acoustic properties of different deformable materials directly in the course of changing their forms. The stand is intended for estimation of the strength and plasticity characteristics of materials during quasistatic tensile, compression, and bending tests synchronized with recording the *stress-strain* diagrams to determine the ultrasound propagation velocity and the ultrasonic wave

Institute of Strength Physics and Materials Science of the Siberian Branch of the Russian Academy of Sciences, Tomsk, Russia, e-mail: lbz@ispms.ru; mvn@ispms.ru; mnikh@yandex.ru. Translated from Izvestiya Vysshikh Uchebnykh Zavedenii, Fizika, No. 5, pp. 36–44, May, 2022. Original article submitted January 20, 2022.

TABLE 1. Achieved Technical Characteristics of the Test Stand

Characteristic	Value
Load testing range	10^2–10^7 N
Accuracy of measuring the ultrasonic waves	$2 \cdot 10^{-4}$
Accuracy of measuring the ultrasound attenuation coefficient	10^{-2}
Accuracy of measuring the displacement vectors	1 μm
Accuracy of measuring the plastic distortion tensor components	10^{-3}
Image registration rate	Up to 50 frames/s
Control computer memory	3 TB

attenuation coefficient as functions of the deformation. Recording and processing of the localized plasticity pattern formed during plastic deformation of the examined material, automatic analysis of the obtained characteristics, and their graphic representation in real time with recording of the results obtained in the control computer memory are also possible.

The operation of the stand was accompanied by synchronized measurement of the plasticity and strength characteristics of deformable materials, observation and analysis of macroscale plastic flow localization patterns, and measurement of small variations in the acoustic properties of the deformable medium directly during deformation. The developed experimental stand included four coordinated units.

The *mechanical unit* was represented by Instron-1185 and Walter Bai AG LFM-125 testing machines intended for recording the plastic flow curves (*stress-strain* diagrams) of materials and determining their mechanical characteristics.

The *optoelectronic unit* represented an ALMEC-*tv* automated laser measuring complex (developed at the Institute of Strength Physics and Materials Science of the Siberian Branch of the Russian Academy of Sciences [1]) intended for recording of plastic flow localization patterns, reconstructing the field of displacement vectors during deformation, and calculating the plastic distortion tensor components. An Edmund semiconductor laser (635 nm and 3.0 mW) was used to illuminate the sample surfaces, and a Point Grey FL3-GE-50S5M-C CCD camera was used to record the speckle structure of the investigated surface (black-and-white, 5.0 MP, and a Sony ICX655, 2/3 sensor with a maximum resolution of 2592 × 1944).

The *acoustic unit* contained a Rigol DG-1022 generator and a Rigol DS-2072A-S digital oscilloscope and was intended for measuring the propagation velocity and the attenuation coefficient of the Rayleigh waves and of the longitudinal and transverse ultrasonic waves during plastic deformation. Measurements of the ultrasound propagation velocity were reduced to the determination of the transit time of an ultrasonic pulse between the transmitting and receiving transducers. The attenuation was determined from the change of the pulse shape. Pulses with a frequency of 3 MHz were excited by a piezoelectric transducer.

The *control unit* included the personal computer that controlled over the stand operation and synchronized measurement and data accumulation procedures using specially developed software. The main characteristics of the stand are presented in Table 1.

According to the two-component model of localized plastic flow evolution in a deformable material, two wave processes co-exist: the localized plastic flow autowaves responsible for the plasticity and the ultrasonic waves redistributing the elastic stresses. The method of comprehensive study of material properties using the measuring stand allowed their parameters to be recorded simultaneously. In most cases, tests were carried out using flat samples cut from sheets of the alloy under study. The working part of the samples was 5 × 80 mm. The flat sample surface should diffusely scatter light. This requirement is defined by the conditions of observations of the localized plasticity pattern using the speckle-photography method [1].

Initial data on the deformation process were obtained in the form of the *flow stress – time* and *ultrasound propagation velocity – time* dependences using the Instron-1185 or Walter Bai AG LFM-125 test machine and the Rigol DG-1022 generator with the Rigol DS-2072A-S digital oscilloscope, respectively. These dependences were redrawn

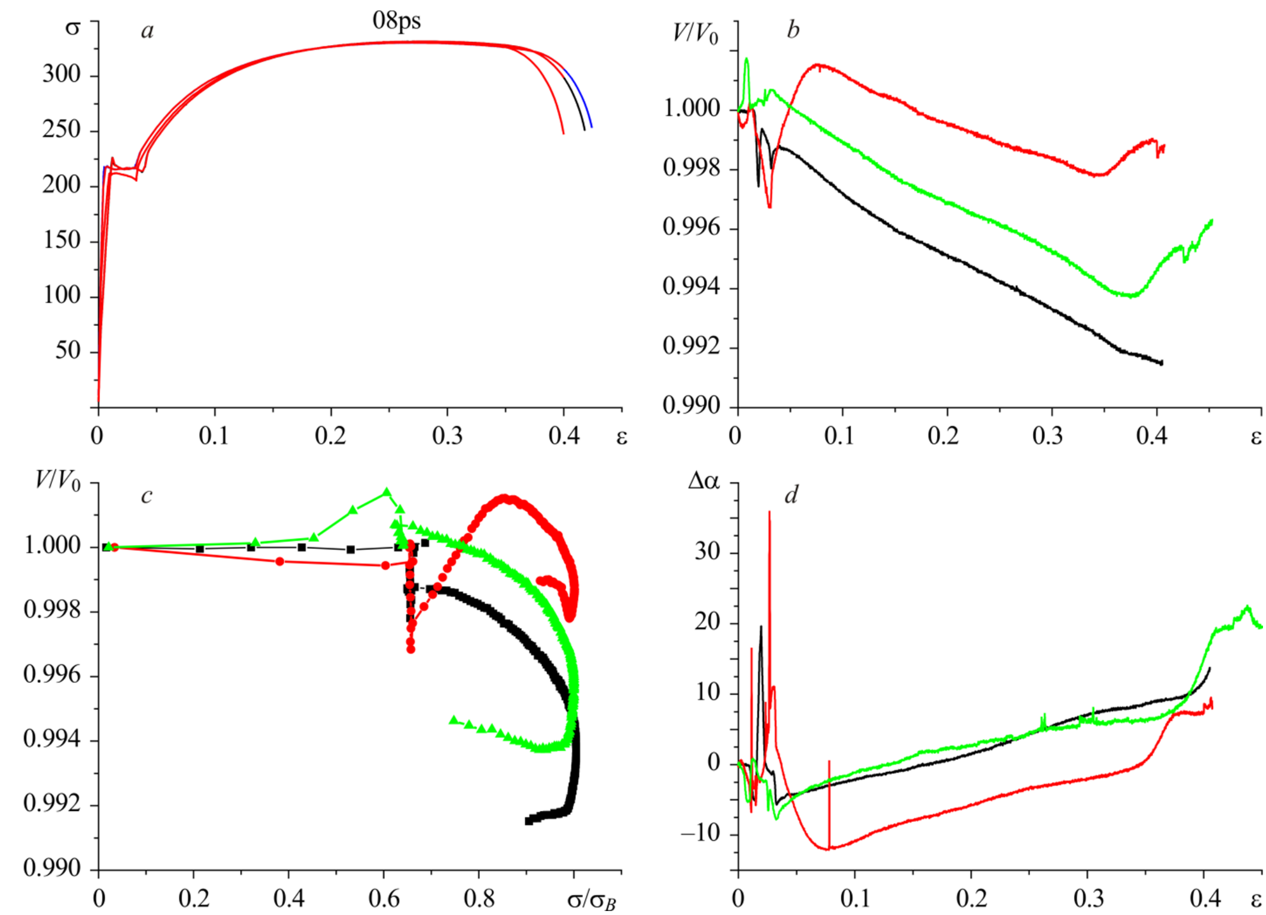

Fig. 1. Stress-strain diagram (*a*), relative changes in the Rayleigh acoustic wave velocity (*b*), relationship between the change in the ultrasound velocity and the time resistance (*c*), and attenuation as a function of the stress (*d*) for the Fe – 0.08 wt.% C (steel 08).

into the *flow stress – strain*, *relative change of the ultrasound velocity – strain*, and *relative change of ultrasound velocity –flow stress* plots and were represented in combined form.

The applicability of the stand for carrying out tests was confirmed by measurements of the acoustic parameters of a deformable medium (the ultrasound velocity and the attenuation coefficient) with simultaneous recording of the localized plasticity patterns formed in materials during plastic flow. These data were obtained in test experiments on tension of flat steel, duralumin, copper, and titanium alloy samples (tensile tests). An example of such dependences is shown in Fig. 1. The plots were drawn automatically using the specially developed software. Sections with characteristic behavior of the dependences of the ultrasound velocity on the strain or stress, for example, with constant velocity values can be identified. These sections unambiguously testify to the implementation of the corresponding law of work hardening.

Thus, the use of the stand makes it possible to supplement significantly information on the standard characteristics of the material, such as the yield point, time resistance, and work hardening coefficient obtained during mechanical tests. As is well known, these characteristics are tentative and poorly reflect the physical nature of the processes observed in solids during plastic deformation [4].

At the same time, comprehensive measurements of the properties using the above-described stand make it possible to interrelate the processes characteristic for structural levels on different scales and hence to use the data on microscopic deformation mechanisms to explain the macroscopic characteristics of the plastic flow process. Formally, the relationship of this type can be manifested through the incorporation of one of the process parameters into the coefficients defining the processes observed on other scale levels. A possibility of elucidation of such relationship is considered below.

2. ESTIMATION OF THE PLASTIC FLOW MICROSCOPIC PARAMETERS FROM RESULTS OF MACROSCOPIC OBSERVATIONS

The estimation of scales of the phenomena defining the plasticity dynamics is the key factor for the construction of any plastic deformation theories, in particular, dislocation ones [5]. The main difficulty in the construction of such theories is the adjustment of dislocation scales characteristic for deformation and work hardening mechanisms to the macroscopic parameters of the deformation processes. Based on the two-component localized plastic deformation model developed in [1] and the idea on the elastoplastic invariant and its consequences, this problem is reduced to the possibility of obtaining microscopic parameters from results of macroscopic observations of the localized plastic flow. The ultrasound propagation velocity is the informative parameter characterizing the metal structure and its change upon plastic deformation.

At first, it makes sense to consider the data on the acoustic properties of the undeformed metal, in particular, polycrystalline aluminum. In this case, as shows experiment [1], the sound velocity is the function of the grain size δ of the form

$$V_S \approx V_0 - \kappa\delta^{-1/2}, \tag{1}$$

linearized in the well-known Hall coordinates $V_S - \delta^{1/2}$ [4]. A possible reason for the decrease in the sound velocity in polycrystals in comparison with single crystals can be grain boundary sliding in a variable elastic ultrasonic wave field that, in particular, causes the occurrence of internal friction maxima at grain boundaries in polycrystalline aluminum [4, 5]. From Eq. (1) rewritten in the form

$$V_0 - V_S = V_t\left(\frac{L}{\delta}\right)^{1/2}, \tag{2}$$

where we have used the replacement $\kappa = V_t \cdot L_{st}^{1/2}$ and denoted by V_t the transverse ultrasonic wave velocity, the structural parameter $L_{st} \approx 10^{-8}$ m can be obtained close in value to the coherent scattering region size in aluminum determined by the x-ray method [1]. This parameter characterizes the crystal lattice of the undeformed material.

To analyze the possibilities for application of the acoustic characteristics of plastic deformation, we take advantage of the quadratic equation $\omega = \omega(k) = \omega_0 + \alpha(k - k_0)^2$ for the variance of the localized plasticity autowave [1, 3, 6]. These data were obtained by recording the localized plasticity patterns in polycrystals with different grain sizes, which makes it possible to analyze the characteristics of the localized plasticity autowaves as functions of the grain sizes. Based on this, the plots $\omega(\delta)$ and $k(\delta)$ were obtained shown in Fig. 2.

Their linear character allows us to consider that $\omega \sim \delta$ and $k \sim \delta$, and for dimensional reasons, taking into account the important role of the elastoplastic invariant, to obtain for the frequency

$$\omega = \frac{D_\varepsilon}{L^3}\delta \tag{3}$$

and for the wave number

$$k = \frac{1}{L^2}\delta. \tag{4}$$

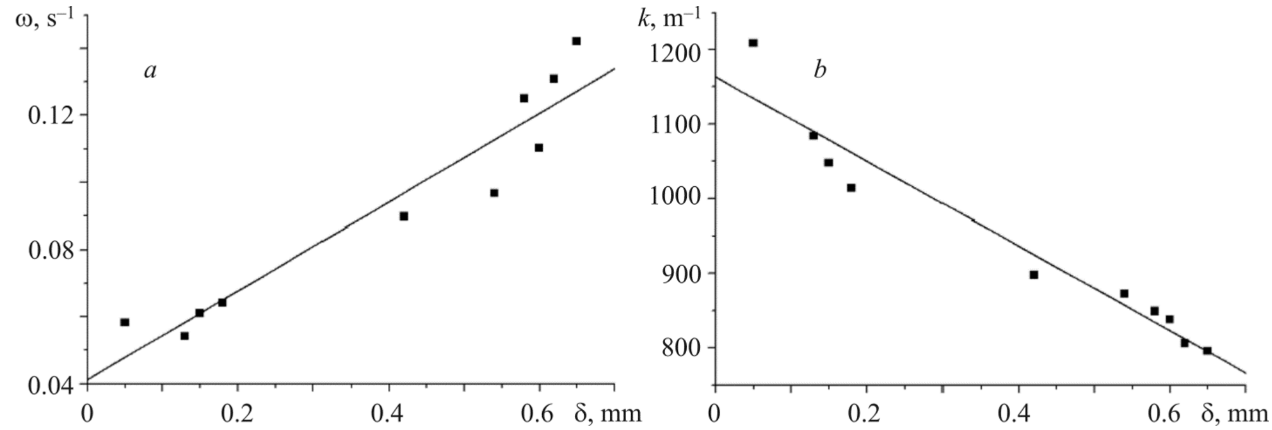

Fig. 2. Dependences of the frequency (*a*) and wave number (*b*) of localized plasticity autowaves in polycrystalline aluminum on the grain sizes.

Based on the data presented in [1, 3], we obtain that the coefficient $D_\varepsilon = d/dt\left(\rho_{md}^{-1}\right)$ is determined by the mobile dislocation density ρ_{md} and has the dimension m^2/s. Simple calculations from formulas (3) and (4) give $L \approx 0.9{\cdot}10^{-3}$ m. This value is close to the grain size in aluminum at which the dependences of some properties on the grain sizes changes [3] and a minimum arises in the dispersion curve when the phase and group phase velocities of plasticity autowaves became equal.

As already established [2], plastic deformation of materials is accompanied by small, but still measurable changes in the ultrasound propagation velocity. The autocirculating method of exact measurement of this parameter convenient for these purposes was described previously [2]. As was established, the velocity changes correlated with plastic flow stages, which was convincingly illustrated by the dependences $V_t(\varepsilon)$ and $V_t(\sigma)$ established during tension of Al samples. An analysis of the general dependence $V_t(\varepsilon,\sigma)$ shown in Fig. 3 for different stages of the polycrystalline aluminum plastic flow showed that $V_t = \mathrm{const}$ at the linear work hardening stages, the dependence $V_t(\varepsilon)$ is *N*-shaped and has three stages, and the plot of the dependence $V_t(\sigma)$ has three rectilinear sections in which the relationship

$$V_t = V_0 + \xi\sigma \tag{5}$$

holds true, where the constants V_0 and ξ differ for different stages of the dependence. Since the coefficient ξ changes its sign during plastic flow, it should depend on the characteristic of the deformation process behaving analogously. The set of these characteristics for the examined plastic deformation problem is limited; however, it is well known that the mobile dislocation density ρ_{md} extremely depends on the strain, and its time derivative should change its sign [1].

The use of mobile dislocations as the density characteristic is defined by the fact that changes in the ultrasound propagation velocity described by Eq. (5) are observed only during deformation rather than when the test machine has been stopped. This indicates the direct relationship between the ultrasound velocity changes and the deformation processes, that is, the dislocation motion. Obviously, the dimension of the coefficient ξ in Eq. (5) is m^2·s·kg^{-1}. Considering in addition that the elastic wave propagation velocity in a substance is related to its density ρ_0, the analysis of dimensions gives

$$\xi \approx \frac{L_i}{\rho_0 D_\varepsilon}\,. \tag{6}$$

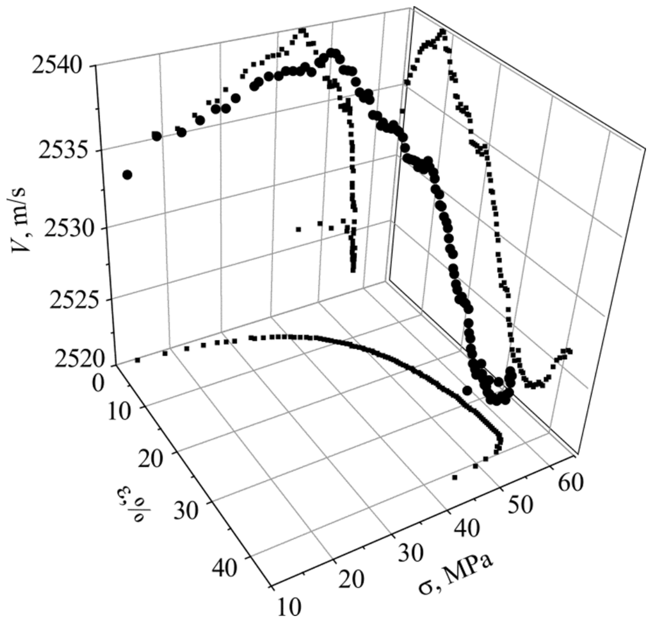

Fig. 3. Curve illustrating the deformation stages and the dependence of the Rayleigh wave velocity on the strain.

The parameter L_i here determines the spatial scale of the plastic deformation mechanism (the characteristic size of the deformation inhomogeneity region), Eq. (6) relates the discrete change of the coefficient ξ to the transition of the process on the other scale level, and the transport coefficient D_ε defines the change of the ξ sign upon plastic deformation. The constant tilts of the sections in the dependence $V_t(\sigma)$ is reached when $L_i / D_\varepsilon = \text{const}$.

The changes in the ultrasound propagation velocity in Figs. 1 and 3 described by Eq. (5) are interesting by a discrete character of changes of the coefficient ξ along the plastic flow curve. According to the above-stated reasons, this suggests that this is caused by changes of L_i values during plastic deformation. If $D_\varepsilon = \text{const}$, then estimating the tilt coefficients with the accuracy up to the sign for three sections of the dependence $V_S(\sigma)$ for Al, we obtain $L_1 \approx 0.3 \cdot 10^{-3}$ m, $L_2 \approx 0.9 \cdot 10^{-3}$ m, and $L_3 \approx 1.1 \cdot 10^{-3}$ m for three stages of this dependence, that is, $L \approx 10^{-3}$ m. This is close in value to the estimate obtained above from the dispersion dependence and apparently, indicates a significant contribution of the grain boundary processes to the deformation. Introducing the wave resistance of the medium $Z_w = V_t \rho_0$, Eq. (5) can be reduced to the form

$$\Delta Z_w = Z_w - Z_{w0} = \left(\frac{L_i}{D_\varepsilon} \right) \sigma . \tag{7}$$

From this it follows that the wave resistance of the material within each stage of the process changes in proportion to the flow stress, but the rate of change at different stages is defined by the internal scales L_i, that is, by the parameters of the internal structure of the material formed at each stage of the deformation process [6, 7].

3. PREDICTIVE CAPABILITIES OF THE LOCALIZED STRAIN ANALYSIS

Equation (5) describing the relationship between the ultrasound velocity and the applied stresses can be used to estimate the strength characteristics of the material by the nondestructive method. Indeed, having introduced the

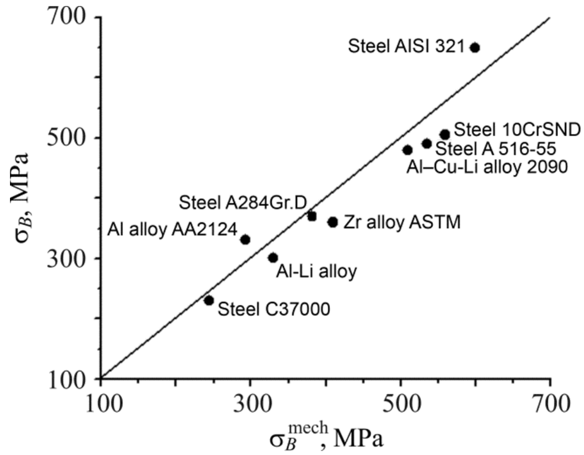

Fig. 4. Correlation between σ_B and σ_B^{mech}.

variables V_t / V_t^* and σ/σ_B, where V_t^* is the sound velocity in the undeformed material and σ_B is the time resistance, we reduce Eq. (5) to the form

$$\frac{V_t}{V_t^*} = \kappa_i + \alpha_i \frac{\sigma}{\sigma_B}, \tag{8}$$

where i = 1, 2, 3 is the stage number, and the constants κ_i and α_i depend on the material type and are determined experimentally. From Eq. (8) it follows that

$$\sigma_B = \frac{\alpha_i}{V_t / V_t^* - \kappa_i} \sigma. \tag{9}$$

Obviously, this relationship can be used to estimate the time resistance σ_B by measuring the value $\delta V_t = V_t - V_t^*$, that is, the changes in the sound velocity when the flow stress increased by σ. The σ_B values calculated from Eq. (9) and the values σ_B^{mech} obtained by standard mechanical testing are linearly correlated, and the correlation coefficient reaches ~0.94, so that we can consider that

$$\sigma_B \approx \sigma_B^{\text{mech}} \tag{10}$$

with the accuracy sufficient for practical purposes.

Relationship (9) was studied for a number of industrial alloys in different structural states. These data are shown in Fig. 4. They suggest that the correlation obtained can provide the basis for the method of determining such characteristic of the material, as the time resistance without sample destruction. It is obvious that according to formula (9), for this purpose it is sufficient to determine the change in the ultrasound propagation velocity under low plastic stress $\hat{\varepsilon}$ (experiments showed that $\hat{\varepsilon} \approx 10^{-2}$ is sufficient for these purposes) and to calculate the time resistance from formula (9). The experimental verification confirmed the sufficient accuracy of this method.

The ideas on the autowave character of the localized plastic deformation developed above are focused on observations of the evolution of the localized plasticity pattern. From this point of view, of particular interest is the predestruction stage when the deformation centers become mobile again. The kinetics of motion of the localized

TABLE 2. Coefficients of Eq. (12) and Calculated Coordinates of the Place and Time of Sample Destruction

Alloy →	1	2	3	4	5	6	7	8	9
$\alpha\cdot 10^3$, s	1.07	2.7	3.83	1.32	4.89	0.83	7.23	4.63	1.95
$\alpha_0\cdot 10^3$, mm/s	6.39	–4.78	8.14	–1.27	9.66	–1.07	–0.60	–17.33	–13.84
X^*, mm	6.0	–1.8	2.1	–1.0	2.0	–1.3	–0.1	–3.7	–7.1
t^*, s	1134	4370	1981	2408	624	2007	938	866	1433

plasticity centers at this stage appears more complex compared to that observed at the stage of linear work hardening, when all centers move with the same velocities forming the phase autowave. The complex character of motion at the predestruction stage is highlighted by the data [1] from which it follows that the localized plasticity autowave collapses at this stage.

At the predestruction stage, the dependences of the locations of localized deformation centers on time $X(t)$ are linear; after extrapolation, they converge to the point with the coordinates (X^*, t^*), forming a bunch of straight lines. The velocities of separate centers remain constant. Obviously, this is possible if these velocities are consistent from the very beginning of the predestruction stage. Only one of all centers the location of which already during formation corresponds to the localization of the future macroscopic neck, remains. Typically, this center that has appeared still at the stage of parabolic work hardening remains almost motionless until destruction, but the deformation in it gradually increases during the flow process decay in other centers.

In order that bunches of straight lines $X(t)$ can be formed, it is necessary that the velocities of motion of the centers depend linearly on the coordinates of the place of their origin ξ, that is, the relation

$$V_{aw}(\varsigma) = \alpha\varsigma + \alpha_0 \tag{11}$$

must be fulfilled, where α and α_0 are empirical constants, and the coordinate ς is counted from the motionless localization center ς^*. The similarity of $X(t)$ diagrams for all investigated materials at the predestruction stage allows us to consider that the processes follow a single scenario provided by automatic setting of relation (11) for the velocities of motion of the centers in the deformable sample as functions of the coordinates of their places of origin ς in the sample at the stage of the localized plasticity autowave collapse corresponding to the predestruction stage.

The constants α and α_0 defined for the alloys under study are presented in Table 2. The coordinates of the bunch centers calculated from the formulas

$$X^* = \alpha_0\alpha^{-1} \text{ and } t^* = t_0 + \alpha^{-1} \tag{12}$$

(t_0 is the time of the beginning of the predestruction stage) that define the place and time of viscous destruction of samples are also presented in the table. This means that formulas (12) can be used to predict these parameters with acceptable accuracy. The prediction procedure is reduced to the following operations. First it is necessary to choose several initial points of the $X-t$ diagrams corresponding to the collapse of the autowave pattern.

Then taking into account that the dependences $X(t)$ are linear, their graphic extrapolation toward the intersection point should be performed, the coordinates of which will give the required destruction place and time. This method was successfully used to control over changes of the form of the zirconium alloy during cold rolling of thin-walled pipe blanks for fuel elements of nuclear reactors [8] and allowed us to prevent the destruction of the blanks at the finishing stages of the technological rolling process.

Results of comparison of the calculated and experimentally fixed X^* and t^* values for some alloys are given in Table 3. From these data, it follows that the proposed method of predicting the destruction place and time allows acceptable estimates of the main destruction characteristics to be obtained. As to the time period of destruction

TABLE 3. Comparison between the Calculated and Experimentally Determined Blank Destruction Coordinates and Times

Alloy	Base alloy				
	Aluminum	Titanium	Vanadium	Magnezium	Zirconium
X^*_{exp}/X^*_{calc}	28/26	39/40	39/40	7.5/7	15/15
t^*_{exp}/t^*_{calc}	4380/4370	2520/2408	630/624	2150/2007	980/938

prediction, its localization and time can be predicted 5−6 min before the event, which is quite acceptable for many modes of the processing of metals by pressure [8].

CONCLUSIONS

The experimental data presented above have shown that observations of the macroscale localized plasticity patterns allow one to obtain additional information on the microscopic plastic flow mechanisms. This can be done by possible estimation of the corresponding macroscale phenomena. The dislocation theory has developed sufficient number of models of the deformation phenomena, but it is most often difficult to link them to macroscopic laws of actual form changing. In this situation, the observation of the localized plasticity patterns using comparatively simple methods can become irreplaceable for the construction of such unified models and theories considering the multiscale deformable medium.

The application of autowave ideas to the nature of the plastic flow makes it possible to formulate the plasticity criteria required for the applied branch of plasticity mechanics. It seems likely that the most evident and informative characteristic of the material deformability without destruction is the form of the localized plasticity pattern. Its *in situ* observation is possible using adapted optoelectronic equipment and big computing resources. At the same time, measuring of the ultrasound propagation velocity during plastic deformation is a much more simple operation and can be used in actual manufacturing. In addition, the existence of a practically unambiguous relationship between the forms of the localized plasticity patterns and the dependence of the ultrasound propagation velocity on the flow strain or stress significantly facilitates the choice of the optimal deformation mode.

This work was performed within the framework of the State Assignment No. FWRW-2021-0011 to the Institute of Strength Physics and Materials Sciences of the Siberian Branch of the Russian Academy of Sciences.

REFERENCES

1. L. B. Zuev, Autowave Plasticity. Localization and Collective Modes [in Russian], Fizmatlit, Moscow (2018).
2. M. Kobayashi, Int. J. Plasticity, **26**, No. 1, 107−125 (2010).
3. L. B. Zuev, S. A. Barannikova, V. I. Danilov, and V. V. Gorbatenko, Prog. Phys. Met., **22**, No. 1, 3−57 (2021); DOI: 10.15407/ufm.22.01.003.
4. J. Pelleg, Mechanical Properties of Materials, Springer, Dordrecht (2013).
5. D. Hull and D. J. Bacon, Introduction in Dislocations, Elsevier, Oxford (2011).
6. V. I. Nekorkin and V. B. Kazantsev, Int. J. Bifurc. Chaos, **12**, No. 11, 2421–2434 (2001).
7. S. A. Barannikova and Yu. V. Li, Russ. Phys. J., **63**, No. 5, 731–737 (2020).
8. O. Bocharov, S. Zavodchikov, V. Belov, *et al.*, in: Proc. 14th Int. Symp. ASTM "Zirconium in the Nuclear Industry," West Conshohoken (2005), pp. 248–263.